ELSEVIER

Journal of Organometallic Chemistry 501 (1995) 211–218

Journal of Organometallic Chemistry

Zirconocenophane dichlorides with di- and trisiloxane-bridged ring ligands: crystal structure of *rac*-[1,1,3,3-tetramethyldisiloxane-diyl-bis(3-tert-butyl-η^5-cyclopentadienyl)zirconium(IV) dichloride] ☆

Jens Gräper [a], Gino Paolucci [b], R. Dieter Fischer [a,*]

[a] *Institut für Anorganische und Angewandte Chemie der Universität Hamburg, Martin-Luther-King-Platz 6, D-20146 Hamburg, Germany*
[b] *Dipartimento di Chimica, Università di Venezia, Calle Larga S. Marta 2137, I-30123 Venezia, Italy*

Received 20 April 1995

Abstract

The three novel zirconocenophane dichlorides $[\{O(Me_2SiC_5H_4)_2\}ZrCl_2]$ (**3**), $[\{O(Me_2SiC_5H_3\text{-}^tC_4H_9)_2\}ZrCl_2]$ (**4**) and $[\{Me_2Si(OMe_2SiC_5H_4)_2\}ZrCl_2]_n$ (**5**) have been prepared and characterized by ^1H NMR spectroscopy. According to a successful single-crystal X-ray study, **4** crystallizes from *n*-hexane as a racemic mixture with exclusively 1,3-disubstituted cyclopentadienyl ligands and Cl_2 centres oriented transoid to the O atoms. **4**: monoclinic; space group $P2_1/c$, $a = 1167.7(2)$, $b = 1590.2(2)$, $c = 1491.3(3)$ pm; $\beta = 104.64(2)°$; $R = 0.061$ ($R_w = 0.058$). In solution (room temperature), all three complexes are fluxional; moreover the NMR spectrum of **4** displays the resonances of two isomers (25 : 1). According to a mass spectrometry study of **5**, the B^2/E-coupled scan of the molecular ion M^+ ($m/z = 494$) indicates at least four "parent" fragments with $509 \leqslant m/z \leqslant 1275$, suggesting here dinuclear or even trinuclear precursors.

Keywords: Zirconocene; Siloxane; Structure

1. Introduction

Ansa-metallocenes containing two siloxane-bridged cyclopentadienyl ligands offer an interesting alternative to systems with aliphatic C_nR_{2n} bridges [1,2] or various heteroatomic tethers, e.g. $C_mR_{2m}XC_nR_{2n}$ [3]. We have demonstrated recently [4] that organolanthanoid complexes of the type $[\{O(Me_2SiC_5H_4)_2\}LnCl]_n$ (Ln = Pr (**1**) or Yb (**2**)) with tetramethyldisiloxane-bridged ring ligands display variable conformational rigidity depending on the temperature and the solvent. Conformational or configurational flexibility is likely to influence also the frequently experienced catalytic activity predominantly of Group 4 metallocenes. In view of the particular importance of zirconocene derivatives, we describe in the following the three siloxane-bridged Zr complexes: $[\{O(Me_2SiC_5H_4)_2\}ZrCl_2]$ (**3**), $[\{O(Me_2SiC_5H_3\text{-}^tBu)_2\}ZrCl_2]$ (**4**) and $[\{Me_2Si(OMe_2SiC_5H_4)_2\}ZrCl_2]_n$ (**5**). While **3** is the Zr homologue of the already reported Ti complex $[\{O(Me_2SiC_5H_4)_2\}TiCl_2]$ (**6**) [5], **5** is the first example involving two cyclopentadienyl ligands interlinked by a trisiloxane chain.

2. Synthesis and general properties of 3–5

Complexes **3**, **4** and **5** were prepared by reacting $ZrCl_4$ with the respective salts $K_2[O(Me_2SiC_5H_4)_2]$ (**7**) [4], $K_2[O(Me_2SiC_5H_3\text{-}^tBu)_2]$ (**8**) and $K_2[Me_2Si(OSiMe_2C_5H_4)_2]$ (**9**) in tetrahydrofuran (THF). Complexes **8** and **9** were obtained by reacting $(SiMe_2Cl)_2O$ with $K[C_5H_4\text{-}^tBu]$, and $(SiMe_2OCl)_2SiMe_2$ with $Na[C_5H_5]$

☆ Dedicated to Professor Herbert Schumann on the occasion of his 60th birthday.

* Corresponding author.

0022-328X/95/$09.50 © 1995 Elsevier Science S.A. All rights reserved
SSDI 0022-328X(95)05643-2

Table 1
List of the six principally possible different isomers of non-fluxional **4**, including characteristic ^{1}H NMR features

Isomer (non-fluxional)	Mutual orientation of O atom and the following		^{1}H NMR pattern expected for the following		
	$ZrCl_2$ bisector axis	CMe_3 group	CMe_3	$SiMe_2$	C_5H_3SiC
rac (1)	Transoid	—	2 singlets	4 singlets	2 ABX patterns
rac (2)	Cisoid	—	2 singlets	4 singlets	2 ABX patterns
meso (1)	Transoid	Transoid	1 singlet	2 singlets	1 ABX pattern
meso (2)	Transoid	Cisoid	1 singlet	2 singlets	1 ABX pattern
meso (3)	Cisoid	Transoid	1 singlet	2 singlets	1 ABX pattern
meso (4)	Cisoid	Cisoid	1 singlet	2 singlets	1 ABX pattern

(1 : 2) respectively and subsequent reduction of the resulting cyclopentadienes with elemental potassium. The ^{1}H NMR spectrum of **8** (solvent, THF-d_8) indicates the presence one positional isomer only (vide infra; Table 4). 1,3-ring substitution is most likely in view of the appearance of two ring-δ(CH) bands at 823 (s) and 905(m) cm^{-1} in the IR spectrum of **8** which are characteristic of one "isolated" and two adjacent ring H atoms [6]. Unlike for $Na_2[Me_2Si(C_5H_3Me)_2]$ and the corresponding Ti(IV) complex [7], the considerable space demand of both ring substituents in **8** is expected to dictate a preference of the 1,3-isomer [8]. Attempts to isolate **5** just in analogy to the syntheses of **3** and **4** has led to a solid containing, in accordance with its ^{1}H NMR spectrum and the elemental analysis, about 25% of the Zr-free ligand as an impurity. Here, only a special treatment of the crude product afforded analytically pure **5** with a reasonably high yield.

The new complexes **3** (white) and **4** (faintly yellowish-green) are air-stable solids, while pure **5** results as a white paste-like material. In the ^{1}H NMR spectra of **3** and **5** the ring protons give rise to clean AA'XX' resonance patterns. In contrast, the ring protons of **4** display two similar ABX patterns of very different relative intensity (about 25 : 1). This intensity ratio turned out to be maintained for all portions of the product successively obtained by fractional crystallization at −30°C.

In view of the expected asymmetrical position of the disiloxane bridge (with respect to the Cl–Zr–Cl plane) [4,5], **4** may in principle adopt four different (non-fluxional) configurations (Table 1). Simple model considerations predict that all *meso* configurations will suffer more of intramolecular steric congestion (e.g. owing to their eclipsed *tert*-butyl groups) than the two racemic forms, suggesting qualitatively the following sequence in configurational stability:

$$rac(1) \geqslant rac(2) > meso(2) \geqslant meso(4) > meso(1) \approx meso(3)$$

Nevertheless, intramolecular ligand rearrangement processes rapid on the NMR time scale may not be ruled out, involving either reorientation of the organic ligand in total [5] or at least a "local" inversion of the bridging C(ring)$SiMe_2SiOSiMe_2$C(ring) fragment (vide infra).

3. Crystal structure of 4

The crystallographic X-ray analysis of a crystal of square prismatic shape harvested from a concentrated solution of **4** in *n*-hexane indicates the presence of molecules of the racemic mixture, *rac*(1), only (Table 1), in accordance with the suggestion that *rac*(1) is sterically most favoured and might thus occur in the highest concentration. Data of particular relevance for the X-ray study are given in Table 2. Fig. 1 presents a view of the molecular structure of the (*S.S*)-enantiomer of *rac*(1) [9], and Table 3 some selected distances and bond angles, respectively. As in **2** [4] and **6** [5], the disiloxane bridge is again disposed asymmetrically, its

Table 2
Summary of crystal data and details of data collection and refinement for **4**

Formula	$C_{22}H_{36}Cl_2OSi_2Zr$
M (g mol^{-1})	534.83
Crystal system	Monoclinic
Space group	$P2_1/c$
a (pm)	1167.7(2)
b (pm)	1590.2(2)
c (pm)	1491.3(3)
β (°)	104.64(2)
V (10^6 pm^3)	2679.3(8)
Z	4
D_c (g cm^{-3})	1.326
F(000)	1112
Temperature (K)	293
Diffractometer	Syntex $P2_1$
Radiation λ (pm)	70.9261
μ (Mo Kα) (mm^{-1})	0.710
Scan technique	$2\theta-\theta$ scan
2θ range (°)	$4.5 < 2\theta < 60.0$
Number of reflections	8764
Number of reflections in refinement	4318
Number of refined parameters	254
Goodness of fit	1.61
Weighting scheme	$[\sigma^2(F)+0.0005F^2]^{-1}$
Limit of significance	$[\lvert F_o\rvert > 4\sigma(F_o)]$
R	0.0608
R_w	0.0583

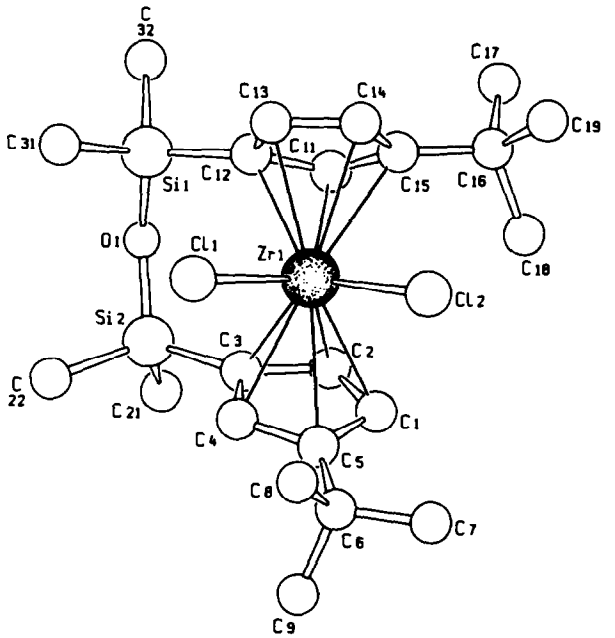

Fig. 1. SCHAKAL plot of the molecular structure of the (S.S)-enantiomer of 4 with atomic numbering scheme

Table 3
Selected interatomic distances (bonding and non-bonding) (pm) and bond angles (°) in **4**

Interatomic distances			
Zr(1)–Cl(1)	244.5(2)	Zr(1)–Cl(2)	243.4(2)
Zr(1)–C(12)	245.4(5)	Zr(1)–C(3)	247.9(4)
Zr(1)–C(15)	258.4(5)	Zr(1)–C5	265.2(5)
Zr(1)–Cent(1)	223.9(3)	Zr(1)–Cent(2)	221.8(3)
Si(1)–O(1)	164.2(4)	Si(2)–O(1)	161.7(4)
Si(1)–C(12)	186.3(5)	Si(2)–C(3)	186.8(5)
Si(1)–C(31)	184.2(9)	Si(2)–C(21)	185.0(6)
C(5)–C(6)	152.0(9)	C(15)–C(16)	153.9(9)
C(2)···C(11)	309.0(7)	C(3)···C(12)	344.0(7)
C(1)···C(15)	408.6(7)	C(4)···C(13)	472.0(7)
C(5)···C(14)	512.7(7)	Zr(1)···O(1)	402.8(5)
C(6)···plane(1)	20(2)	C(16)···plane(2)	24(3)
Si(2)···plane(1)	32(2)	Si(1)···plane(2)	28(3)
Bond angles			
Cl(1)–Zr(1)–Cl(2)	98.1(1)	Cent(1)–Zr(1)–Cent(2)	132.8(1)
Si(1)–O(1)–Si(2)	138.1(3)	C(3)–Si(2)–O(1)	112.1(2)
Cent(1)–C(5)–C(6)	7.1(3)	Cent(2)–C(15)–C(1)	68.9(3)
Cent(1)–C(3)–Si(2)	9.8(2)	Cent(2)–C(12)–Si(1)	9.3(3)

oxygen atom lying "transoid" to the Cl_2 centre. The two five-membered ring ligands are eclipsed, although non-parallel, the presence of two bulky substituents per ring leading to five different (instead of three), non-bonding C–C distances for the five pairs of opposite-lying ring carbon atoms (see Table 3). The Zr–C(ring) distances display also considerable alterations, the two (non-equivalent) alkylated C-atoms being most remote from, and the two silylated C-atoms closest to, the metal atom [11]. All four ring substituents (including the atoms C(6), C(16), Si(1) and Si(2)) lie outside the best-ring planes in *exo* positions (i.e. away from Zr). The Si(1)–O–Si(2) angle of **4** resembles that of **6** (141.5° [5]) in being significantly smaller than in common open-chain siloxanes (142–156° [12]). The

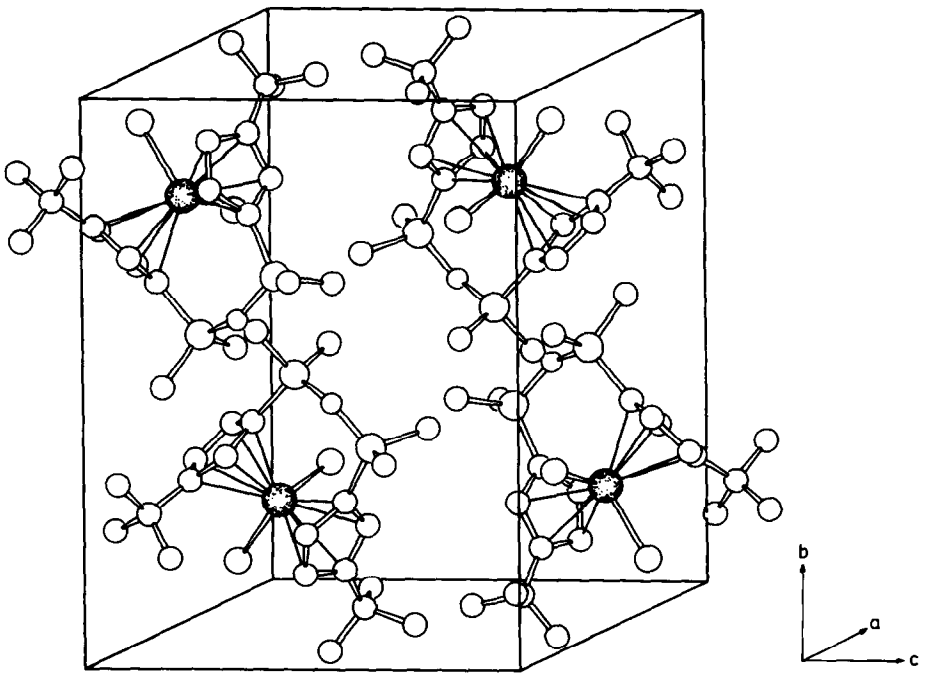

Fig. 2. Unit cell of **4**. The upper pair of molecules are (*S.S*) and the lower pair of molecules (*R.R*) enantiomers [9] (the circles representing Zr atoms are dotted).

cent(1)–Zr–cent(2) angle of **4** exceeds the corresponding angles of for example $\{(CH_2)_3(C_5H_4)_2\}ZrCl_2$ (129.5° [13]) and *rac*-$\{Me_4C_2(C_5H_3CMe_3)_2\}ZrCl_2$ (124.8° [2]) considerably, while neither the Cl–Zr–Cl' angles nor the Zr–Cl distances of these three complexes display notable variations. Interestingly, all Si–C distances in **4** are quite similar, although the carbon atoms are either sp^2 or sp^3 hybridized; moreover, the Si–C distances in **4** are shorter than the usual Si–C distances in polysiloxanes (188–123 pm [12]). Most of the structural irregularities mentioned may be due to steric congestion owing to the presence of two comparatively bulky substituents per ring ligand. Molecular packing seems, nevertheless, optimal for the racemic mixture of *rac*(1) (Fig. 2). Intra- and inter-Zr · · · O distances are too long (636.7 pm or greater) to suggest any genuine Zr–O interaction.

4. NMR spectroscopy

Solutions of the new complexes **3–5**, as well as of the potassium salts **7–9**, were subjected to high resolution ^1H NMR spectroscopy mainly at room temperature; the resulting NMR data are collected, together with those already reported for **6** [5], in Table 4. The resonance pattern of **3** corresponds, at least down to −40 °C, to that of **6** in that for example only one methyl singlet appears, suggesting for **3** the same rapid (on the NMR time scale) ligand reorientation as proposed by Curtis et al. [5] for **6**. This behaviour contrasts notably with that of the related, apparently more compactly structured lanthanoid complexes **1** and **2** [4]. The 360 MHz spectrum of **4** reveals the appearance of two individual, similarly featured spectra of considerably different intensities (about 25 : 1 (Fig. 3)). Each spectrum could primarily be correlated with one of the anticipated *meso* forms, *meso*(1) to *meso*(4) (Table 1) as only one CMe_3 proton single occurs. The crystallographic result described above according to which the racemic mixture, *rac*(1), is most likely to reach the highest concentration in solution, and the well-confirmed fluxionality of **3** may, however, advocate for an assignment of the more intense spectrum to a likewise fluxional racemic form. Following Curtis et al. [5], the corresponding ligand reorientation process of **4** is schematically depicted in Fig. 4. Both *rac*(1) and *rac*(2) should pass the same, severely strained type of intermediate. While this mode of fluxionality would lead to virtually identical CMe_3 groups, the prochiral nature of each $-SiMe_2O$ fragment in **4** still justifies the expectation of two different siloxy methyl resonances, in spite of the complete pairwise interconversion: $CH_3^a \rightleftarrows CH_3^b$ as suggested by Fig. 4. Thus, under fluxional conditions, the ^1H NMR spectra

Table 4
Survey of observed ^1H NMR data for **3–5** and their precursors **7–9** (all measurements at room temperature)

Compound	δ (ppm)		
	C_5H_4–C_5H_3 [a]	$Si(CH_3)_2$	$C(CH_3)_3$
$[\{O(Me_2SiC_5H_4)_2\}ZrCl_2]$ (**3**) (solvent, CD_2Cl_2)	6.98 (t, 4H, J_{HH} = 2.5 Hz) 6.50 (t, 4H, J_{HH} = 2.5 Hz)	0.37 (s, 12H)	
$[\{O(Me_2SiC_5H_3\text{-}^tC_4H_9)_2\}ZrCl_2]$ (**4**) (solvent, C_6D_6)	6.68 (t, 2H, J_{HH} = 2.2 Hz) [b] 6.63 (t, 2H, J_{HH} = 2.2 Hz) [b] 6.39 (dd, 2H, J_{HH} = 2.2, 2.9 Hz) [b] 6.81 (t, 2H, J_{HH} ≈ 2.2 Hz) 6.74 (t, 2H, J_{HH} ≈ 2.2 Hz) 6.20 (dd, 2H, J_{HH} ≈ 2.2; 2.9 Hz)	0.38 (s, 6H) [b] 0.30 (s, 6H) [b] 0.36 (s, 6H) 0.27 (s, 6H)	1.32 (s, 18H) [b] 1.47 (s, 18H)
$[\{Me_2Si(OSiMe_2C_5H_4)_2\}ZrCl_2]$ (**5**) (solvent, CD_2Cl_2)	6.71 (t, 4H, J_{HH} = 2.4 Hz) 6.62 (t, 4H, J_{HH} = 2.4 Hz)	0.34 (s, 12H) 0.13 (s, 6H)	
$[\{O(Me_2SiC_5H_4)_2\}TiCl_2]$ (**6**) (solvent, $CDCl_3$ [5])	6.48 (t, 4H, J_{HH} = 2.5 Hz) 6.26 (t, 4H, J_{HH} = 2.5 Hz)	0.12 (s, 12H)	
$K_2\{O(Me_2SiC_5H_4)_2\}$ (**7**) (solvent, THF-d_8 [4])	5.80 (m, 4H) 5.57 (m, 4H)	0.20 (s, 12H)	
$K_2\{O(Me_2SiC_5H_3\text{-}^tC_4H_9)_2\}$ (**8**) (solvent, THF-d_8)	5.75 (m, 3H) 5.50 (m, 3H)	0.18 (s, 12H)	1.33 (s, 18H)
$K_2\{Me_2Si(OSiMe_2C_5H_4)_2\}$ (**9**) (solvent, THF-d_8)	5.74 (m, 4H) 5.55 (m, 4H)	0.20 (s, 12H) 0.08 (s, 6H)	

[a] All triplets are, strictly speaking, pseudotriplets.
[b] Data belonging to the spectrum of the most abundant isomer (see text).

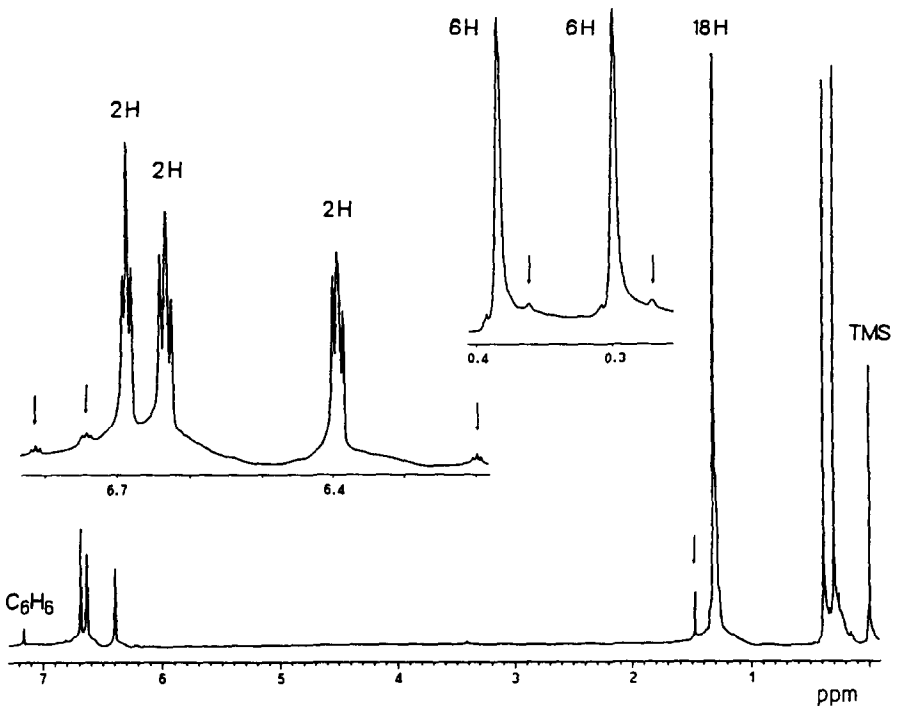

Fig. 3. ^{1}H NMR spectrum of **4** (C_6D_6, 360 MHz). The vertical arrows indicate resonances of the less abundant isomer (see the text).

of the racemic and the *meso* forms of **4** should look surprisingly similar.

Interestingly, Brintzinger and coworkers [2] have reported ^{1}H NMR results reflecting a corresponding rapid reorientation of two C_2Me_4-interlinked and extra-substituted cyclopentadienyl ligands in complexes of the general type $C_2Me_4(3\text{-R-}C_5H_3)_2MCl_2$. In the ring proton ABX spectra of these systems, however, the two pseudotriplets of the α-protons (referred to the *ipso*-carbon atom) appear at higher fields than the double doublet of the β-proton. The "reversed" sequence displayed by **4** resembles more that observed by Klouras and Köpf [7] and Köpf and Klouras [14] for related ansa-metallocenes. In contrast, the less intense spectrum of **4** which could be best ascribed to a *meso* form gives rise to a larger $|\Delta(\alpha, \beta)|$ value (i.e. the difference between the centres of the α and the β resonances) than does the spectrum of the main component. Brintzinger and coworkers [2] have found that for their ansa-metallocenes the value of $|\Delta(\alpha, \beta)|$ of the *meso* form always exceeds that of the racemic form. Unlike **4** and the C_2Me_4-bridged metallocene dihalides, racemic ethylenebis(1-indenyl)zirconium(IV)dichloride as well as its bis-tetrahydrogenated derivative display only one singlet for the eight methylene protons [15] in spite of the prochirality of each–CH_2C fragment.

The NMR spectrum of **5** agrees with the composition of the organic ligand and reflects, moreover, a molecule with virtually two mirror planes perpendicular to each other. Thus, in spite of the high oxophilicity of zirconium, the trisiloxane bridge must be considered as chemically intact and strongly fluxional. ^{1}H NMR spectroscopy is, however, unable to help to distinguish here between molecules of the primarily anticipated ansa-metallocene type and oligomeric or even polymeric systems involving metal bridging instead of chelating $Me_2(OSiMe_2C_5H_4)_2$ ligands. Interestingly, the two new trisiloxane-bridged lanthanoid complexes $\{Me_2Si(OMe_2SiC_5H_4)_2\}$ PrCl(THF)] and $[\{Me_2Si(OMe_2Si\text{-}C_5H_4)_2\}YbCl]_2$ [16] have turned out to be paste-like and a viscous oil respectively as well.

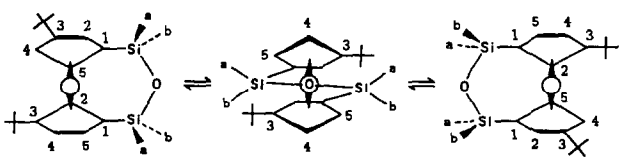

Fig. 4. Schematic representation of the intramolecular ligand reorientation process of disiloxane-bridged metallocenes adapted (following Curtis et al. [5]) to **4**. Cl atoms are not shown for clarity.

5. Mass spectrometry of 5

In view of the non-crystalline consistency of **5** which strongly disfavours facile access to single crystals suit-

able for X-ray crystallography, **5** was subjected to a mass spectrometry (MS) study. Somewhat surprisingly, **5** turned out to be considerably more volatile than for example, **2** [4] in that a good survey spectrum became already possible at a chamber temperature of 100 °C (for **2**, 300 °C). All metal-containing fragments of $M^{\cdot+}$ with $I_{rel} > 5$ of the survey spectrum are listed in Table 5. While the MS is dominated by the basis peak of $M^+ - Me^{\cdot}$ (= A) and $M^{\cdot+}$ (secondmost intense) a number of much weaker peaks corresponding to significantly higher m/z values than for $M^{\cdot+}$ appear as well. While the intensities of these peaks were too low to manage B/E-linked scan studies to determine the corresponding daughter ions, some B^2/E-linked scan experiments focusing on eventual parent ions of $M^{\cdot+}$ were possible. According to these studies, $M^{\cdot+}$ fragments appear to result from at least four parent ions with $m/z = 1275$, 902, 535 and 509 (Fig. 5). Although these findings do advocate for the existence of at least one oligomeric parent species, the available data are too poor to focus on any distinct molecule. Simply the fact that eventually the heaviest parent ion has $m/z = 1275$ which is close to that of a trinuclear species ($3 \times 494 = 1482$) suggests that a trinuclear complex, probably with metal bridging $Me_2Si(OSiMe_2C_5H_4)_2$ ligands, might be involved.

6. Experimental section

All operations were carried out under pure nitrogen, adopting throughout familiar Schlenk techniques. IR spectra were recorded on the Perkin–Elmer model 1720 (Fourier transform technique; KBr pellets), and ^{1}H NMR spectra on the Bruker instruments WP 80 (80 MHz) or AM 360 (360 MHz). MS studies were carried out as described in [4], and details of the single-crystal X-ray study are collected in Table 2.

Table 5
Mass spectrometry data for **5** (normal mass spectrometry; m/z values considering the isotopes ^{28}Si, ^{35}Cl and ^{90}Zr only; *EI*, 70 eV; probe temperature, about 100 °C).

Fragment	Formula	m/z	I_{rel} (%)
$M^{\cdot+}$	$C_{16}H_{26}Si_3O_2ZrCl_2$	494	25
$M^{\cdot+}-Me^{\cdot}$ (**A**)	$C_{15}H_{23}Si_3O_2ZrCl_2$	479	100
$M^{\cdot+}-Cl^{\cdot}$ (**B**)	$C_{16}H_{26}Si_3O_2ZrCl$	459	21
(**A**)–$Cl^{\cdot}$	$C_{15}H_{23}Si_3O_2Zr$	444	8
(**B**)–$Cl^{\cdot}$	$C_{16}H_{26}Si_3O_2Zr$	424	12
(**A**)–C_5H_4SiMe	$C_9H_{16}Si_2O_2ZrCl_2$	372	5
(**B**)–Me_2SiCl	$C_{14}H_{20}Si_2O_2Zr$	366	7
(**A**)–$(Me_2SiO)_2$	$C_{11}H_{11}SiZrCl_2$	331	7
(**A**)–(MeSiCl–O–$SiMe_2$O) (**C**)	$C_{12}H_{14}SiZrCl$	311	25
(**C**)–$Me^{\cdot}$	$C_{11}H_{11}SiZrCl$	296	8
(**C**)–$Cl^{\cdot}$	$C_{12}H_{14}SiZr$	276	8
(**C**)–MeSiH	$C_{11}H_{10}ZrCl$	267	17

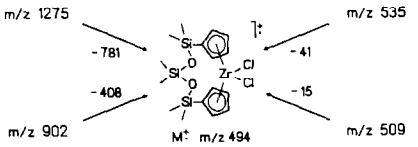

Fig. 5. Parent ions of M^+ of (mononuclear) **5** as detected by B^2/E-linked scan studies.

6.1. Preparation of $(SiMe_2Cl)_2O$, $Me_2Si(OSiMe_2Cl)_2$, $K_2[O(Me_2SiC_5H_4)_2]$ (7) and $K_2[Me_2Si(OSiMe_2C_5H_4)_2]$ (9)

The syntheses of the two dichlorosiloxanes as well as of $K_2[O(Me_2SiC_5H_4)_2]$ (**7**) have been described in [4]. To prepare $K_2[Me_2Si(OMe_2SiC_5H_4)]$ (**9**), a solution of 5.00 g (4.91 ml = 0.018 mol) of $Me_2Si(OSiMe_2Cl)_2$ in 30 ml of tetrahydrofuran (THF) was added to a solution of 3.5 g (0.040 mol) of NaC_5H_5 in 20 ml of THF. After stirring overnight at room temperature, filtration and solvent evaporation, a light-yellow viscous oil is obtained which is redissolved in about 20 ml of THF. After addition of 1.41 g (0.036 mol) of finely divided potassium, stirring (12 h at room temperature), filtration and solvent evaporation, 5.7 g of a wax-like colourless solid are obtained (yield; 94%). ^{1}H NMR: see Table 4, IR (KBr pellets): ν 3071 m, 3055 m, 3039 m, 2956 m, 2898 m, 1671 w, 1588 w, 1472 sh, 1439 s, 1411 m, 1349 m, 1259 vs, 1192 s, 1082 sh, 1061 sh, 1073 vs, 1018 sh, 905 m, 856 s, 820 sh, 793 vs, 733 s, 709 s, 701 m, 676 m, 580 w, 558 m, 529 w, 479 w, 440 s cm^{-1}. Details of the conversion of **9** into **5** will be outlined in a forthcoming paper on corresponding lanthanoid complexes.

6.2. Preparation of $K_2[O\{Me_2Si(3\text{-}C_4H_9)C_5H_3\}_2]$ (8)

A solution of 3.53 g (22.0 mmol) of $K(^tC_4H_9)$ in 30 ml of THF is added dropwise, within about 45 min (room temperature), to a solution of 2.03 g (10.0 mmol) of $(SiMe_2Cl)_2O$ in about 80 ml of THF contained in a 250 ml three-necked flask equipped with a dropping funnel and reflux cooler. The reaction mixture is then kept at about 45 °C for 3 h and stirred for another 2 days at room temperature. After filtration and complete solvent evaporation, the colourless solid is suspended in about 60 ml of petrol ether. After filtration and solvent evaporation in vacuo, 3.20 g of $O\{Me_2Si(3\text{-}C_4H_9)\text{-}C_5H_4\}_2$ are isolated from the yellow filtrate as a viscous oil. The latter is redissolved in 50 ml of THF and reacted with about 1.50 g (38.3 mmol) of finely divided potassium. Notable H_2 development is observed after warming to 40–45 °C. After overnight stirring, the reaction mixture is gently warmed before filtration. After solvent evaporation from the light-grey filtrate and drying of the residue at about 40 °C, 3.63 g of a greyish

white wax-like product are obtained (yield; 81%; reference, $(SiMe_2Cl)_2O$). ^1H NMR: see Table 4. IR(KBr): ν 3050 m, 2954 s, 2899 m, 2860 m, 1641 w, 1581 w, 1516 w, 1462 s, 1408 s, 1361 s, 1333 m, 1250 vs, 1189 s, 1169 m, 1130 sh, 1085 vs, 1053 vs, 1031 vs, 963 m, 937 m, 924 m, 905 w, 823 s, 788 vs, 719 m, 685 s, 658 m, 593 m, 544 w, 477 w, 433 m cm^{-1}.

6.3. Preparation of $[\{O(Me_2SiC_5H_4)_2\}ZrCl_2]$ (3)

1.601 g (6.85 mmol) of $ZrCl_4$ cooled to −78°C (dry ice–EtOH bath) are united dropwise (0.5 h) with 25 ml of THF. The finally clear solution is warmed slowly to 50 °C, whereafter a solution of 2.321 g (6.85 mmol) of **7** in 20 ml of THF is added under stirring for 1 h. The white-yellow suspension is stirred for another 3 h at 50 °C and for 2 days at room temperature. After filtration (D4 frit) and washing of the residue with about 20 ml of *n*-hexane, solvent evaporation (in vacuo) from the colourless filtrate and drying (high vacuum), 2.05 g of colourless microcrystalline **3** are obtained (71% yield). Anal. Found: C, 37.61; H, 4.83; Cl 16.72; Si 10.81; Zr, 22.56. $C_{14}H_{20}OCl_2Si_2Zr$ calc.: C, 39.79; H, 4.77; Cl, 16.78; Si, 13.29; Zr, 21.58%. ^1H NMR: see Table 4. IR (KBr): ν 3095 m, 3082 m 2956 m, 2901 m, 1616 m, 1596 sh, 1447 m, 1420 m, 1410 m, 1371 m, 1317 m, 1259 vs, 1185 s, 1180 sh, 1079 sh, 1073 sh, 1043 vs, 1024 vs, 943 m, 925 m, 905 s, 840 sh, 827 sh, 801 vs, 705 m, 672 m, 648 m, 632 m, 569 m, 435 m cm^{-1}.

6.4. Preparation of $[O\{Me_2Si(3\text{-}^tC_4H_9)C_5H_3\}_2ZrCl_2]$ (4)

A solution of 1.030 g (2.29 mmol) of **8** in about 40 ml of THF is added dropwise within 1 h to a gently warm (40–50 °C) solution of 0.526 g (2.26 mmol) of $ZrCl_4$ in 40 ml of THF. The light-yellow suspension is stirred for another 6 h at 40 °C, and subsequently for 3 days at room temperature. After solvent evaporation and extraction of the solid yellow residue with about 100 ml of *n*-hexane (5 h; vigorous stirring), the clear yellow solution (obtained after filtration and partial solvent evaporation to about 10 ml) is cooled to −30 °C overnight. The resulting fine precipitate is washed with a little cold (−30 °C) *n*-hexane, and the mother liquor is treated correspondingly again. The total yield is 436.2 mg (36%) of a faintly yellowish-green powder. Anal. Found: C, 48.78; H, 6.83; Zr, 17.53. $C_{22}H_{36}OCl_2Si_2Zr$ calc.: C, 49.41; H, 6.78; Zr, 17.06%. ^1H NMR: see Table 4. IR (KBr): ν 3092 m, 2957 s, 2903 m, 2866 m, 1580 w, 1488 m, 1463 m, 1392 m, 1363 m, 1338 m, 1254 m, 1089 s, 1063 s, 1025 s, 982 m, 962 m, 924 m, 823 s, 811 s, 792 s, 780 m, 703 m, 678 m, 669 m, 666 sh, 657 sh, 657 sh, 593 m, 574 m, 481 w, 454 w, 436 w, 424 m cm^{-1}.

Table 6
Atom coordinates and isotropic temperature factors for **4**, with estimated standard deviations in parentheses

	x ($\times 10^{-4}$)	y ($\times 10^{-4}$)	z ($\times 10^{-4}$)	U_{eq} (pm^2)
Zr(1)	16385(4)	19450(3)	34164(3)	441(1)
Cl(1)	22182(16)	24070(13)	20299(10)	890(7)
Cl(2)	3845(13)	7659(11)	27440(12)	866(7)
Si(1)	22989(14)	42571(10)	40950(12)	623(6)
Si(2)	43893(12)	31069(10)	48983(11)	610(5)
O(1)	34702(31)	38778(22)	48381(28)	687(15)
C(1)	27095(41)	8066(32)	45255(30)	475(16)
C(2)	29150(39)	15889(31)	49596(29)	437(15)
C(3)	36175(38)	20922(30)	45082(31)	458(16)
C(4)	38295(39)	15693(33)	38035(31)	482(17)
C(5)	33049(41)	7715(32)	37987(32)	479(16)
C(6)	34925(47)	190(35)	32236(35)	577(19)
C(7)	27689(64)	−7327(44)	33903(55)	1040(37)
C(8)	32015(69)	2057(49)	22038(39)	1028(34)
C(9)	47967(54)	−2228(44)	35612(50)	918(31)
C(11)	8636(39)	28733(28)	44803(32)	448(16)
C(12)	11982(41)	33875(31)	38089(32)	486(16)
C(13)	3678(45)	32235(34)	29608(37)	593(20)
C(14)	−4285(44)	26035(36)	31067(35)	582(19)
C(15)	−1360(40)	23903(30)	40498(32)	466(16)
C(16)	−8681(44)	18689(34)	45739(38)	574(20)
C(17)	−12912(55)	24817(40)	52157(46)	790(28)
C(18)	−1299(53)	11874(38)	51590(45)	756(26)
C(19)	−19273(54)	14725(49)	39056(48)	971(33)
C(21)	52247(61)	30045(41)	61251(45)	983(30)
C(22)	53766(55)	33381(47)	41412(54)	1014(35)
C(31)	26430(62)	46398(45)	30267(53)	1095(38)
C(32)	16729(57)	50957(40)	46697(51)	918(29)

6.5. X-ray crystallography of 4

Single crystals were grown form a concentrated *n*-hexane solution at about −30 °C and the crystal was fixed in a 0.5 mm Lindemann capillary. The program RAUM [17] was favourably used to determine the correct space group. Heavy-atom positions were located by means of three-dimensional Patterson synthesis, followed by difference Fourier and least-squares refinements as well as by an empirical absorption correction (program DIFABS [18]). All non-hydrogen atoms were anisotropically refined, and a fixed C–H distance of 96 pm was adopted using a collective temperature factor. A residual electron density of 1.00 electrons $Å^{-3}$ could be located within a radius of about 80 pm around the Zr atom. Atomic coordinates and isotropic temperature factors are collected in Table 6. Interatomic distances and bond angles (Table 3) were determined using the programs SHELXLS [19] and PLATON 90 [20,21].

Acknowledgement

The authors (R.D.F. and J.G.) greatly appreciate the financial support by the Bundesministerium für Forschung und Technologie, Bonn.

References and notes

[1] For examples with m = 2, see for example [2] and J.M. Nelson, H. Rengel and I. Manners, *J. Am. Chem. Soc., 115* (1993) 7035; with m = 3: H. Schnutenhans and H.H. Brintzinger, *Angew. Chem., 91* (1979) 837; *Angew. Chem., Int. Edn. Engl., 18* (1979) 777; with *m* = 5: C. Qian, C. Ye, H. Lu and Y. Li, *J. Organomet. Chem., 263* (1994) 333; C. Qian, Z. Xie and Y. Huang, *Inorg. Chim. Acta., 139* (1987) 195.

[2] S. Gutmann, P. Burger, H.-U. Hund, J. Hofmann and H.-H. Brintzinger, *J. Organomet. Chem., 369* (1989) 343.

[3] For examples with *m* = *n* = 2 and X = 0 or NR', see C. Qian, Z. Xie and Y. Huang, *J. Organomet. Chem., 323* (1984) 285; H. Schumann, J. Loebel, J. Pickardt, C. Qian and Z. Xie, *Organometallics, 10* (1991) 215; C. Qian and D. Zhu, *J. Organomet. Chem., 445* (1993) 79.

[4] J. Gräper, R.D. Fischer and G. Paolucci, *J. Organomet. Chem., 471* (1994) 87.

[5] D.M. Curtis, J.J. D'Errico, D.N. Duffy, P.S. Epstein and L.B. Bell, *Organometallics, 2* (1983) 1808.

[6] M. Hesse, H. Meier and B. Zeeh, *Spektroskopische Methoden in der anorganischen Chemie*, G. Thieme, Stuttgart, 1979, p. 79.

[7] N. Klouras and H. Kopf, *Monatsh. Chem., 112* (1981) 887.

[8] *Organikum, Organisch-Chemisches Grundpraktikum*, VEB Deutscher Verlag der Wissenschaften, Berlin, 1981, p. 375.

[9] In contrast with different notations occasionally used for a distinct metallocene enantiomer [2], the rules consistent with the (*R*, *S*) nomenclature [10] have been followed throughout.

[10] (a) R.C. Cahn, C. Ingold and V. Prelog, *Angew. Chem., 78* (1966) 413, *Angew. Chem., Int. Edn. Engl., 5* (1966) 385; (b) K. Schlögl, *Fortschr. Chem. Forsch., 6*(3) (1966); E. Heilbronner, V. Hofmann, K. Schäfer and G. Wittig, (eds.), Springer, Berlin, p. 479; (c) R.L. Haltermann, *Chem. Rev., 92* (1992) 965.

[11] Strictly speaking, the distance Zr–C(2) (247.1(4) pm) is almost negligibly shorter than the distance Zr–C(3) (247.9(4) pm).

[12] A.F. Wells, *Structural Inorganic Chemistry*, Clarendon, Oxford, 5th edn., 1984, pp. 997.

[13] C.H. Saldarriaga-Molina, A. Clearfield and I. Bernal, *J. Organomet. Chem., 80* (1974) 79.

[14] H. Köpf and N. Klouras, *Z. Naturforsch., 38b* (1983) 321.

[15] F.R.W.P. Wild, M. Wasiucionek, G. Huttner and H.H. Brintzinger, *J. Organomet. Chem., 288* (1985) 63.

[16] J. Gräper, *Dissertation*, Universität Hamburg, 1993.

[17] G. Fendesak, RAUM, Universität Hamburg, Hamburg, 1989.

[18] H. Maelger, DIFABS, Universität Hamburg, Hamburg, 1991; N. Walker and D. Stuart, *Acta Crystallogr. Sect. A, 39* (1983) 158.

[19] *SHELXTL PLUS 4.21/V*, Siemens Analytical X-Ray Instruments, Madison, WI, 1990.

[20] A.L. Spek, *Acta Crystallogr. Sect. A, 46* (1990) C31.

[21] Further details about the X-ray struture may be obtained from the Fachinformationszentrum Karlsruhe, Gesellschaft für wissenschaftlich-technische Information mbH, D-76344 Eggenstein-Leopoldshafen (Germany), on quoting the depository number CSD 58089, the names of the authors, and the journal citation.